Neuronal mechanism of mirror movements caused by dysfunction of the primary motor cortex in the monkeys

Fumiharu Tsuboi

Department of Physiological Sciences
School of Life Science
The Graduate University for Advanced Studies
(SOKENDAI)

2009

Abstract

Mirror movements (MMs) are often observed in patients with some congenital neurological diseases and hemiplegic after stroke. In the latter case, MMs are supposed to reflect some aspects of recovery process. Therefore, understanding the neuronal mechanism of MMs should contribute as a measure of rehabilitative training, but their mechanism is not clearly understood from indirect evidence obtained in human case studies. Here we found that reversible inactivation of the primary motor cortex (M1) induced MMs in the unaffected hand during voluntary grasping with the affected hand in monkeys. Using this animal model, we investigated the origin of MMs after unilateral dysfunction of M1. We found the MMs thus induced were completely abolished by additional blockade of the contralateral M1. Detailed analysis of EMG revealed that mirror EMG activity in the unaffected hand is temporally correlated but its amplitude sometimes does not parallel with that of the homonymous muscle in the affected hand, which suggests that the enhanced activation of the intact M1 leading to MMs was not derived from the signal from the affected M1. Rather, the present finding suggests that common drive of bilateral M1 from higher order structures and reduction in inter-hemispheric inhibition concomitantly caused the MMs via enhanced activity of the intact M1.

Abbreviations

AP = adductor pollicis; BB = biceps brachii; CNS = central nervous system; ECU = extensor carpi ulnaris; EDC = extensor digitorum communis; ED2.3 = extensor digit 2.3; FCU = flexor carpi ulnaris; FDI = fast dorsal interosseous; FDS = flexor digitorum superficialis; FPB = flexor pollicis brevis; ICMS = intracortical microstimulation; L- = left; MMs = mirror movements; MUS = muscimol; M1 = primary motor cortex; PL = palmaris longus; PMv = ventral premotor cortex; R- = right; TB = triceps brachii;

Contents

Introduction····1

Methods····5

Results···· 12

Identification of hand area of M1····12

Induction of mirror movements by muscimol injection into right M1····12

EMG analysis of mirror movements····14

Blockade of mirror movements by additional injection of muscimol into left M1··17

Effect of additional injection of left PMv····18

Discussion····19

Characteristics of mirror movements induced by reversible inactivation of M1···19

Possible mechanism of mirror movements following dysfunction of M1·····20

Figure legends····23

Figures····27

Acknowledgements····49

Introduction

Mirror movements (MMs) are involuntary and unnecessary movements that accompany voluntary movements of the opposite side of the body. MMs often occur in distal upper limb muscles. MMs are known to be observed during infancy but disappear with development (Mayston et al., 1999). But MMs are also known to occur in adulthood in the following cases; patients with hereditary neurological diseases such as Klippel-Feil syndrome (Farmer, 1990), X-linked Kallmann's syndrome (XKS) (Shibasaki and Nagae, 1984; Mayston et al., 1997; Krams et al., 1997; Farmer et al., 2004), familial Parkinson's disease (Li et al., 2007) and congenital hemiplegia (Nass, 1985) or hemiplegic patients caused by stroke (Nelles, 1998; Kim et al., 2003).

Among these, MMs often reflects the deficiency of motor functions after the stroke (Nelles, 1998) and can be a useful measure of recovery process after brain and spinal cord injury. Therefore, understanding the neural mechanism of MMs will contribute to setting the roadmap of rehabilitative training.

Several lines of studies have been devoted to clarify the neuronal pathways responsible for induction of mirror movements in human patients using transcranial magnetic stimulation (TMS) or functional magnetic resonance imaging (fMRI) techniques (Mayston et al., 1999; Kim et al., 2003; Ueki et al., 2005; Verstynen et al.,

2007) but their conclusions vary depending on the neurological disorders that the subjects suffer from and on the experimental procedures by which they were examined.

In a recent review by Carson (Carson, 2005), the neuronal mechanisms of MMs were classified into four different categories (Fig.1); the first is “uncrossed ipsilateral pathway”. It has been reported that in the patients of X-linked Kallmann’s syndrome, pathological movements are associated with activity in fast-conducting ipsilateral corticospinal axons whose cell bodies share common synaptic input with those of the crossed corticospinal projections (Mayston et al., 1997). The second is “bifurcating bilateral cortico-motoneuronal projections”. It has been proposed that MMs observed in patients of Klippel-Feil syndrome are caused by aberrant branching of the crossed corticospinal fibers in the spinal cord that innervates motoneurons of the ipsilateral side in addition to the normal innervations of the contralateral motoneurons (Farmer et al., 1990). The third is “bilateral cortical activation”. In this case, the activity of the motor cortex was enhanced on the contralateral side to the hemisphere used for voluntary movements, which led to induction of MMs via the crossed corticospinal projections. The MMs in infants (Mayston, 1999) and hemiplegic patients due to stroke were proposed to be caused by such mechanism, which was caused by dysfunction of inter-hemispheric inhibition via the corpus callosum. The fourth is “the common inputs

from the upstream cortical regions such as the supplementary motor area (SMA) or the premotor area (PM) project to the bilateral primary motor cortex (M1) and leads to enhancement of bilateral cortical activity". In this case, the MMs are induced via the crossed corticospinal projection from the M1 contralateral to the hand of MMs, as well as the third possibility. However, it is usually difficult to differentiate the third and fourth possibility in the experimental studies on human cases. Especially, it is often difficult to conclude whether cortical activation, observed in fMRI, was the cause of the MMs or results of the MMs by re-afferent effect.

Until now, studies to clarify the neural origin of MMs have been performed only in human subjects and no study has been performed on animal models. Animal models, especially those using macaque monkeys, should be valuable to clarify the neural mechanisms because they have similar structure of the brain and body, and because experimental manipulations are possible in these animals, which can never be performed on human subjects (Darian-Smith and Ciferri, 2005; Lemon and Griffiths, 2005; Courtine et al., 2007; Isa et al., 2007; Nishimura et al., 2009). These experimental manipulations include controlling the location and timing of the lesion, electrical and/or pharmacological manipulations of neural activities, additional lesion and single unit recordings, etc. If we could establish useful animal model of MMs, it will surely

contribute to understand the neural mechanism or generation of MMs. In the present study, first, we tested whether a macaque monkey with motor deficiency caused by acute reversible blockade of M1 can be a model of MMs. Then as the second step, using this model, we analyzed the neural mechanism of MMs by additional reversible blockade of neural activities.

Material and Methods

Subjects

Three Macaca fuscata monkeys (Monkey M: male 6.2 kg, Monkey T: male 4.5 kg, Monkey Y: female 4.7 kg) were used in this study. The experiments followed the NIH Guideline for the Principles of Laboratory Animal Care and the guideline of the Ministry of Education, Culture, Sports, Science and Technology of Japan, and were approved by the committee for animal experimentation of the National Institute of Natural Sciences.

Behavioral test

The monkeys were trained to be seated on a monkey chair in the laboratory and reach, grasp and retrieve a small piece of sweet potato or apple (7 mm cubic) through a narrow cylindrical tube (diameter 5 cm) using the left hand, while the right hand was restricted. The food piece was positioned in the center of the tube positioned at the height of their shoulder and at a sagittal distance of 20 cm. Reaching movements started from voluntary pressing of a button (diameter 2 cm) placed on the table 10 cm in front of the left hand of the monkey. After the monkey pressed the button with left hand for 1-3 seconds, the food was put in the tube and then the monkey started reaching for the food piece. The monkey performed this task with self-paced mode, and actually they

performed 50-100 trials during the single session.

Surgical procedures

1. Surgery for EMG recording

After the monkeys became used to the task, they were implanted with bipolar intramuscular EMG electrodes under anesthetized conditions. General anesthesia was initiated by ketamine hydrochloride (10 mg/kg, i.m.) and xylazine (1 mg/kg, i.m.) and then maintained with pentobarbital sodium (Nembutal, 20 mg/kg, i.v.). Supplemental doses of anesthetics were given as needed during surgery. Diclofenac sodium (Voltaren, Novartis, Tokyo) was routinely applied to the anus for analgesia after surgery. EMG activities were recorded from totally 22 muscles of both upper extremities (11 for each, Fig.2), triceps brachii (TB), biceps brachii (BB), extensor digitorum communis (EDC), extensor digit 2.3 (ED2.3), extensor carpi ulnaris (ECU), palmaris longus (PL), flexor carpi ulnaris (FCU), flexor digitorum superficialis (FDS), fast dorsal interosseous (FDI), flexor pollicis brevis (FPB), adductor pollicis (AP). Through chronically implanted pairs of multi-stranded, stainless steel wires (Cooner Wire, Chatsworth, CA, US) which were subcutaneously tunneled to their target muscles. Circular connectors (MCP-12, Omnetics, Minneapolis, MN, US) were anchored to the skull.

2. Surgery for electrophysiological mapping and muscimol injection

Before the operation for attaching the cortical chambers, MRI images of the brain were taken under anesthesia introduced by ketamine hydrochloride and xylazine and maintained with pentobarbital sodium as described above to determine the position of attachment.

General anesthetic conditions were the same as surgery for EMG recording. The skull over the bilateral frontal cortices was widely exposed by skin incision. After partial removal of the skull, a pair of delrin chambers were attached to cover each opening. Small titanium-steel screws (diameter 2 mm) were implanted in the skull as anchors. The skull and screws were completely covered with acrylic resin. Two stainless-steel tubes were mounted in parallel over the frontal and occipital lobes and attached to the head plant to fix the head to the experimental setup.

Electrophysiological mapping

After recovery from the surgery, the monkeys were sedated with ketamine (10 mg/kg, i.m.) and seated quietly in a primate chair with their head fixed in a stereotaxic flame attached to the chair. A glass-coated Elgiloy-alloy microelectrode (0.9-1.4 MΩ at 1 kHz) was inserted perpendicularly to the cortical surface using a hydraulic micromanipulator (SM-21, Narishige, Tokyo). Regions in the precentral gyrus were mapped with intracortical microstimulation (ICMS). Each track was separated by 2 mm

or longer. In each penetration, extracellular unit activities were recorded initially, followed by examination of neuronal responses to somatosensory (by passive joint movement or light touch of the skin) and visual stimuli. Subsequently, the monkeys underwent ICMS at the same site. Each pulse had a negative phase followed by a positive phase, with each phase having a duration of 0.2 ms. Stimulus trains (currents less than 50 μA at 333 Hz) were delivered through a constant-current stimulator. The number of pulses per train was 10, 20, 30 or 40. Evoked movements of various body parts were carefully observed. The evoked movements detected by visual inspection were further monitored by direct muscle palpation. In this way, the topographic representation of body parts in the M1 and ventral premotor cortex (PMv) were defined on bilateral sides by the movements of the body parts evoked with the threshold below 40 μA.

Muscimol injection

The somatotopic maps thus constructed were used to determine the injection sites of muscimol. On the day of the injection experiment, ICMS was performed again with a microelectrode and neural recordings at the site chosen for the injection, in order to confirm that the point of injection was actually in the digit area on the topographic map and that the depth of injection was in the gray matter. The microelectrode was then

withdrawn and replaced by a stainless steel microinjection cannula connected to a 10 μl Hamilton microsyringe. The cannula was mounted on the same micromanipulator used for stimulation and recording, so that the needle was inserted into the same track as the microelectrode. The cannula was once lowered to 500 μm below the depth of the site chosen for the injection and subsequently raised again to the correct depth. Muscimol, a $GABA_A$ receptor agonist (volume, 0.4-3.0 μl; concentration, 2.5, 1.25, 0.25 μg/μl, dissolved in 0.1 M phosphate buffer at pH 7.4), was slowly injected by pressure at a rate of 0.2 μl/1 min. The depth chosen for muscimol injection was 3 and 6 mm for M1 (anterior bank of the central sulcus) and 2 and 4 mm for the PMv.

Data collection and analysis

1. Kinematics of hand movements

Two digital video cameras (Panasonic NV-GS50, Osaka, 33 flames/s taken at a shutter speed of 1/1000 sec) were used to record the movements of the left and right hands, respectively. Left hand movements (reach, grasp and retrieve) were taped from a lateral view, and right movements were taped from the top. The digitized flame images were processed by motion capture system (DIPP-Motion XD, DITECT, Tokyo). On the movements of the left hand, the position of the food piece was pointed to define the distance between tip of index finger and food piece and the timing of contact to the food

piece was determined. For both hands, the points of the tip of thumb and index finger were determined and the aperture of each hand was measured. The video images taken by the 2 cameras were merged on the same monitor by using screen-splitting (Panasonic WJ-MS424, Osaka) and synchronized.

2. Experimental protocol

As illustrated in Fig.3, on the day of the experiment, monkeys were seated on a monkey chair, and performed reach and grasp task with the left hand with the right hand constrained. Video recording and EMG recording were performed on separate trials of each session. Each session consisted of 50-100 trials. Muscimol was injected into the digit area of the right M1. One hour after the injection, the test session consisting of 50-100 trials (10 for video and others for EMG recordings) were recorded. After the sessions, the second injection of muscimol was performed in the left M1 or PMv. One hour later, the second recording session was performed. On the next day of the experiments with muscimol injection, the monkeys were just briefly tested whether the effect of muscimol still remains or not. It was confirmed that the effect of muscimol disappeared on the next day.

3. Analysis of EMG activities

EMG of 22 muscles (see above) were sampled at a rate of 5 kHz with high cut

filter of 3kHz and time constant of 0.003 sec. Cross correlation analysis was performed on EMG activities of homonymous muscles in both left and right extremities while the monkey was grasping the food piece with the left hand ("grasping phase") and while the monkey was carrying the food piece to the mouth ("eating phase"). The beginning of the grasping phase was determined by a photoelectric sensor attached to the entrance of the tube. The beginning of the eating phase was determined by the photoelectric sensor placed near the mouth. For both phases, their period was defined as that between 250 ms before and after the detection of the hand. For correlation analysis, the EMG records were re-sampled at a rate of 50 Hz and smoothened at a time constant of 0.2 sec and correlation was calculated on the data of 20 records.

Results

Identification of hand area of M1

The topographic map of motor representation was determined in bilateral precentral motor cortices with ICMS to determine the injection site of muscimol. The position of electrode tracks were first determined by the location of the central sulcus as judged with MRI and surface view of the dura over the cortices. Figure 4 shows the topographic map of M1 and PMv in the three monkeys used in the present experiments. The digit area of M1 (indicated by "D" in the figure) was determined by low threshold induction of digit movements, where the threshold was often less than 10 μA at the most appropriate point of the track. As shown in the figure, the digit area of M1 was distributed over a wide region in the precentral gyrus. However, it was difficult to find the digit area in the PMv. In the present series of experiments, it was detected only in Monkey Y, in which digit movements were induced at high threshold (31-40 μA with 10 pulses) at the bank of the arcuate sulcus (Fig.4).

Induction of mirror movements by muscimol injection into right M1

Fig.5 exemplifies a case in Monkey T in which muscimol injection into the right M1 caused MMs in the right hand. Before injection, no MMs were observed in the right hand while the monkey was grasping the object by precision grip with independent

control of individual fingers of the left hand (Fig.5Aa, Fig.5Ba blue line and Ca). One hour after injection of muscimol into digit area of the right M1, the monkey showed deficiency in precision grip with the left hand as shown in previous studies (Brochier et al., 1999), the monkey could eventually retrieve the food piece but became unable to move the fingers independently and often had to repeat 2 - 3 grasping behaviors before getting the piece out of the tube (Fig.5Ab, Fig.5Bb and Fig.5Cb). Then, as shown in pictures in Fig.5Ab right, MMs occurred in the right hand simultaneously with grasping of the left hand. As exemplified in the kinematic analysis in Fig.5Bb, flexion of the digits in the right hand occurred grasping with the left hand. Thus, partly impaired grasping movements with the left hand accompanied MMs in the right hand. When the examiner pulled the food piece which was pinned to a holder when the monkey grasped it and resisted the retrieval by the monkey, the monkey had to exert stronger force in his left hand to pull out the food piece. Then, MMs became more prominent. Thus, the larger the effort to grasp with the left hand was, the more prominent was the MMs. In addition to the grasping phase, MMs were also observed during the eating phase. When the monkey carried the food piece and released to the mouth, the right hand was expanded simultaneously.

Similarly, MMs were observed in other two monkeys. Monkeys M and T

showed MMs during the eating phase more prominently than the grasping phase, while vice versa in Monkey Y.

EMG analysis of mirror movements

Fig.6 shows the EMG activity of 11 pairs of homonymous muscles of bilateral hands during the reach and grasp task in Monkey T before and after muscimol injection into the digit area of the right M1. As shown in Fig.6A, no clear EMG activity was observed in the right hand during the reach and grasp movements with the left hand, despite weak EMG activity was occasionally observed in the right FDS and ED2.3 during the eating phase.

In contrast, after muscimol injection into the right M1 (Fig. 6B), mirror EMG activity could be observed clearly in some muscle pairs (i) while the monkey was holding the button, (ii) during the grasping phase and (iii) during the eating phase. While the monkey was holding the button, mirror EMG activity was prominent in right PL, FCU, FDS, and weakly in the right FPB. During the grasping phase, mirror EMG activity of right hand became prominent in FPB, ECU and ED2.3. During the eating phase, EMG activity of the right hand was enhanced in BB, FPB, EDC, ECU and ED2.3. Mirror EMG activity was also prominent on the right FDI and AP between the grasping and eating phase, that is, while the monkey was returning the hand to the mouth.

Especially, EMG activity of the right ECU and ED2.3 became stronger during the long period spanning the grasping to eating phase.

In addition, it should be pointed out that the EMG activity of left FPB, one of the prime mover during the grasping phase was almost diminished after muscimol injection, however the EMG activity of the right FPB was much enhanced. This result indicated that overall amount of activity in homonymous muscles do not always parallel, which suggested that cortical activity which evokes muscle activity of the left hand is not the direct source of activation of the right hand muscles (see Discussion).

In Fig.7, the EMG activity of selected muscle pairs of the left hand and right hand during the grasping phase (A) and eating phase (B) are plotted along the X- and Y-axis, respectively for each of the three monkeys to illustrate the temporal pattern of co-activation. After muscimol injection into the right M1, BB and PL of Monkey M changed to co-activation pattern during the eating phase (Fig.7B1b). We could not find muscle pairs which changed clearly to co-activation pattern during the grasping phase in this monkey. Similarly, in Monkey T, EMG activity of BB and FDI changed to co-activation pattern during the eating phase (Fig.7B2b). On the other hand, in Monkey Y, ED2.3, clearly showed switch to the co-activation pattern during the grasping phase (Fig.7A3b), but co-activation pattern could be clearly detected in no muscle pairs during

the eating phase in this monkey.

Fig.8 exemplifies the correlation coefficient with different time lag between selected pairs of the homonymous muscles during the grasping phase (above) and eating phase (below) in Monkey T. We could not observe any sharp peak around the zero-time lag. But as shown in the figure, a broad peak, which was not observed under the control condition, became evident in some muscle pairs such as ECU during the grasping phase and BB during the eating phase after muscimol injection into the right M1.

Fig.9 shows the correlation coefficient of homonymous muscles pairs at the zero-time lag during the grasping phase (A) and eating phase (B) under the control condition and after the muscimol injection into the right M1 in each of the three monkeys. For this analysis, only prime movers of each phase were selected. That is, EDC, ED2.3, ECU, FDS, FDI, FPB and AP were selected for the grasping phase and BB, EDC, ED2.3, FDS, FPD and AP were selected for the eating phase. As shown in the figure, in Monkey M, correlation at the zero-time lag increased in FDI and ED2.3 during the grasping phase, while it increased in all the selected muscle pairs during the eating phase. In Monkey T, correlation at the zero-time lag increased in ED2.3 and ECU during the grasping phase, while it increased in BB, FDS and FPB during the eating phase. In Monkey Y, correlation at the zero-time lag increased in ED2.3, FDI and FPB

during the grasping phase, while it increased in FPB and AP. Thus, larger change in correlation was observed during the eating phase in Monkey M, whereas during the grasping phase in Monkey Y, similarly as in the kinematic analysis and X-Y plot analysis described above. However, the increase in correlation of FPB during the eating phase was the common finding in all the three monkeys.

Blockade of mirror movements by additional injection of muscimol into left M1

To test the possible involvement of left M1 in induction of MMs in the right hand under the present condition, the second injection of muscimol was performed in the digit area of the left M1 about 1 hour after the first muscimol injection into the right M1. Fig.10A shows the movements of the left and right hands during the reach and grasp task with the left hand before the second injection (left; after the first injection) and after the second injection. Fig.10B shows the kinematic analysis. As clearly shown in the figure, after the second injection of muscimol, the movements of the left hand was virtually the same as before the second injection, but MMs in the right hand completely disappeared. This figure illustrates the case of Monkey T but similar observation was obtained also in other two monkeys.

The mirror EMG activity in the right hand also disappeared (Fig.11). The co-activation pattern observed after the first muscimol injection in selected muscle pairs

also disappeared (Fig.12) in all the three monkeys. The broad peak of correlation of activity in homonymous muscles disappeared (Fig.13) and correlation at zero-time lag also tended to decrease after the second injection (Fig.14).

Effect of additional injection of left PMv

To examine possible involvement of the left PMv mediating the command for the MMs, the second muscimol injection was performed in the left PMv in Monkey Y. But no effect was observed on the MMs in the right hand with this manipulation (Fig.15). Temporal pattern of co-activation of EMG activity did not appear to change (Fig.16, 17) and the correlation at the zero-time lag was virtually constant over the second injection (Fig.18).

Discussion

Characteristics of mirror movements induced by reversible inactivation of M1

In the present study, as the first step, we tested whether we can establish an animal model of MMs in macaque monkeys. It was necessary to carefully control the concentration and amount of solution of muscimol; overdose of muscimol resulted severe impairment of movements and knocked down the EMG activity of the left hand, which made it difficult to test the behavior of the animal. On the other hand, shortage of the dose caused virtually no deficit in the movement left hand, which did not induce MMs in the right hand. Accordingly, we had to carefully choose the appropriate dose of muscimol, but in this way we could repeatedly generate the MMs in macaque monkeys by such a reversible blockade of digit area of the M1. Of course, this model is different from human cases of hemiplegia which are usually chronically induced by stroke, most often around the internal capsule. In such cases, not only the motor functions but also the sensory functions are impaired. In addition, there are also many cases of patients without MMs after brain damage and relationship between the location of the damage and occurrence of MMs is not clear as yet (Uttner et al., 2005). In these chronic cases, plastic change in the neural circuits might have happened during the post-injury period, which might also differ from the present experiments in acute induction of MMs. On the

other hand, it is also reported that even in normal human subjects, MMs could be transiently induced when greater effort is required or due to fatigue of the prime mover muscles (Aranyi and Rosler, 2002). Using the TMS, the authors concluded that MMs under such condition was caused by motor irradiation due to reduction in the inter-hemispheric inhibition (Aranyi and Rosler, 2002). In the present study, it was observed that MMs were more prominent when more effort (or force) was required for the monkey to retrieve the food piece. Therefore it is possible that the MMs induced in the present experiments were caused mainly by the increased effort for the animals due to deficiency caused by partial blockade of M1 activity by muscimol.

Despite these concerns, the present animal model of reversible induction of MMs surely gives us an opportunity to analyze the neuronal mechanism of how impairment of M1 activity can induce MMs. Additional experimental manipulations using pharmacological tools and detailed analysis of muscle activation patterns performed in the present study surely give us an opportunity to understand on the mechanism of the MMs in an analytical manner.

Possible mechanism of mirror movements following dysfunction of M1

In the present experiments, the second injection of muscimol into the left M1, which did not cause additional effect on the movement of the left hand, completely shut

down the MMs in the right hand. This was repeatedly confirmed in all the three monkeys. On the other hand, similar blockade of the left PMv caused no effect on the MMs. These results suggested that the enhanced activation of the left M1 mediated the MMs in the right hand. Therefore it is likely that blockade or M1 activity caused enhancement of activation of the contralateral M1. It is highly likely due to reduction in inter-hemispheric inhibition. Thus, the MMs in the present condition are likely due to the possibility 3 or 4 in Carson's proposal (Fig.1; Carson, 2005). Moreover, detailed EMG analysis in the present study gave us suggestion about the likeliness between the possibilities 3 and 4. As shown in Fig.6, the EMG pattern of homonymous muscles did not always show clear mirror image. In some muscle pairs, especially in case of FPB, disappearance of EMG activity of the left hand due to the blockade of right M1 accompanied strong activation of EMG activity on the right side. Such observation cannot be explained by the possibility 3, where the activation of the right M1 was the source of activation of the left M1. Instead, it is more likely as in case of the possibility 4 and schematically drawn in Fig. 19, some higher region sends the commands for the movement to M1 on both sides (more strongly to the right side for the movement of the left hand) but the inter-hemispheric inhibition from the dominant side (right M1) prevents the activation of the left M1 under the normal condition. However, when the

activity of right M1 is impaired, the inter-hemispheric inhibition was reduced and as a result the activation of the left M1 was enhanced in response to the drive from the higher region, which led to induction of MMs. The present results surely contribute to understanding the neuronal mechanism of MMs after stroke and using the MMs as a measure of rehabilitative process in stroke patients.

Figure legends

Fig.1 Possible mechanisms of mirror movements (from Carson, 2005)**. A,** This scheme illustrates the possibility that the facilitatory interactions between the two motor pathways that are evident in the context of voluntary movement of a single limb may be attributable in part to fast-conducting ipsilateral corticospinal axons (ICSA), which fail to cross at the pyramidal decussation, and whose cell bodies share common synaptic input with those of the crossed corticospinal projections (CCSA). **B,** The possibility that the facilitatory interactions between the two motor pathways that are evident in the context of voluntary movement of a single limb may be attributable in part to corticospinal tract neurons (CSN) that branch and project bilaterally to innervate homologous motor pools. **C,** The possibility that the facilitatory interactions between the two motor cortices that are evident in the context of voluntary movements of a single limb may be attributable in part to collaterals of corticospinal neurons, which project from the focal (M11) to the opposite (M12) motor cortex via the corpus callosum (CC). **D,** The possibility that the facilitatory interactions between the two motor cortices that are evident in the context of voluntary movement of a single limb may be attributable in part to common inputs from non-primary (N-P1) motor centers upstream of motor cortex (M11) that are transmitted to the opposite hemisphere (N-P2 and M12) via the corpus callosum (CC).

Fig.2 Muscles with electrodes implanted for EMG recordings. Upper arm muscles: triceps brachii (TB), biceps brachii (BB); forelimb muscles: extensor digitorum communis (EDC), extensor digit 2.3 (ED2.3), extensor carpi ulnaris (ECU), palmaris longus (PL), flexor carpi ulnaris (FCU), flexor digitorum superficialis (FDS); intrinsic hand muscles: fast dorsal interosseous (FDI), flexor pollicis brevis (FPB), adductor pollicis (AP). The EMG of these 11 muscles were recorded on both sides.

Fig.3 Experimental protocol. The schematic drawing of the procedure on the day of the experiment.

Fig.4 ICMS mapping. Somatotopic map in the M1 and PMv on both sides revealed by the ICMS (3 monkeys). Each electrode penetration is represented with a character indicating the body territory activated at the movement threshold. The size of characters indicates the threshold for induction of movements. Annotation of characters and relationship with the threshold are indicated in the inset. The location of muscimol injections are indicated on a surface map of the precentral region with colored filled

circles. The location of the injection sites on both sides are indicated by the same numerals. A. Monkey T, B. Monkey M, C. Monkey Y.

Fig.5 Kinematics of mirror movements before and after the first injection of muscimol. A. Movements of the left hand (left raw) and right hand (right raw) taken simultaneously by sequential video images are shown. The timing relative to the first contact of the index finger to the food piece (time = 0 sec) are indicated on the left. The colored lines (in a. and in b.) connecting the tip of the index finger and thumb indicate the aperture. a. Before the first injection of muscimol. b. One hour after the first injection of muscimol. **B.** The temporal change of apertures of the left (blue line) and right (magenta line) apertures during the reach and grasp task. Zero on the horizontal axis indicates the timing of the first contact of the index finger to the food piece. a. Before the first injection of muscimol, b. One hour after the first injection of muscimol into the right M1. **C.** The temporal relationship of apertures of left and right hands during grasping movements are shown on the X-Y plot (left hand on the horizontal axis and right hand on the vertical axis). Records start from the time = 0 sec (contact of the index finger to the object). The aperture of the left and right hands were normalized against those at time = 0 sec. a. Before the first injection of muscimol into the right M1. b. One hour after the first injection of muscimol.

Fig.6 EMG records during the reach and grasp task before and after the first injection of muscimol. EMG records of 11 pairs of homonymous muscles on both sides during the single trial of reach and grasp task are exemplified. Duration of the button press is indicated with a line. Four dots above the EMG records indicate the timing of the release from the button, insertion of the finger into the tube, extracting the finger from the tube, the hand approaching the mouth. Preparation phase (the monkey was pressing the button), grasping phase and eating phase are hatched with red, purple and green. The mirror EMG appearing in the right hand are indicated with yellow hatch together with the EMG of the left hand. A. Before injection of muscimol, B. One hour after the first injection of muscimol into the right M1.

Fig.7 Temporal relationship of EMG activities of homonymous muscles during the reach and grasp task before and after the first injection of muscimol. Amplitude of rectified EMG activity of the homonymous muscles sampled at 50 Hz are shown on the X-Y plot (left hand on the horizontal axis and right hand on the vertical axis). Records of 20 movements are superimposed. A. Grasping phase, B. Eating phase. 1.

Monkey M, 2. Monkey T, 3. Monkey Y. For each, a. Before injection of muscimol, b. One hour after the first injection of muscimol into the right M1. The nomination of the muscle is indicated in each panel.

Fig.8 Temporal profile of cross-correlation between homonymous muscles before and after the first injection of muscimol. Cross-correlation of EMG activity of ECU for grasping phase (A) and BB for eating phase (B) in Monkey T with different time lag (-0.25 - +0.25 sec). a. Before injection of muscimol, b. One hour after injection of muscimol into the right M1.

Fig.9 Comparison of peak values of cross correlation between homonymous muscles before and after the first injection of muscimol. Correlation coefficient of cross-correlation between the homonymous muscles at time lag zero is plotted for control and one hour after muscimol injection. A. Grasping phase, B. Eating phase. Only prime movers of each phase are indicated. Horizontal broken lines indicate the significance level at 5%. 1. Monkey M, 2. Monkey T, 3. Monkey Y. For each, left. Before injection of muscimol, right. One hour after the first injection of muscimol into the right M1.

Fig.10 Kinematics of mirror movements before and after the second injection of muscimol. a. One hour after the first injection of muscimol into the right M1, b. One hour after the second injection of muscimol into the left M1. A, B, C were illustrated in the same arrangement as Fig.5.

Fig.11 EMG records during the reach and grasp task before and after the second injection of muscimol. A. One hour after the first injection of muscimol into the right M1, B. One hour after the second injection of muscimol into the left M1. Fig.11 was illustrated in the same arrangement as Fig.6.

Fig.12 Temporal relationship of EMG activities of homonymous muscles during the reach and grasp task before and after the second injection of muscimol. a. One hour after the first injection of muscimol into the right M1, b. One hour after the second injection of muscimol into the left M1. Fig.12 was illustrated in the same arrangement as Fig.7.

Fig.13 Temporal profile of cross-correlation between homonymous muscles

before and after the second injection of muscimol. a. One hour after the first injection of muscimol into the right M1, b. One hour after the second injection of muscimol into the left M1. Fig.13 was illustrated in the same arrangement as Fig.8.

Fig.14 Comparison of peak values of cross correlation between homonymous muscles before and after the second injection of muscimol. For each, left. One hour after the first injection of muscimol into the right M1, right. One hour after the second muscimol injection into the left M1. Fig.14 was illustrated in the same arrangement as Fig.9.

Fig.15 The effect of muscimol injection into PMv; photographs. a. Before injection of muscimol, b. One hour after the first injection of muscimol into the right M1, c. One hour after the second injection of muscimol into the left PMv. A, B were illustrated in the same arrangement as Fig.5.

Fig.16 The effect of muscimol injection into PMv; EMG. A. Before injection of muscimol, B. One hour after the first injection of muscimol into the right M1, C. One hour after the second injection of muscimol into the left PMv. Fig.16 was illustrated in the same arrangement as Fig.6.

Fig.17 The effect of muscimol injection into PMv; temporal relationship of EMG activities. a. Before injection of muscimol, b. One hour after the first injection of muscimol into the right M1, c. One hour after the second injection of muscimol into the left PMv. Fig.17 was illustrated in the same arrangement as Fig.7.

Fig.18 The effect of muscimol injection into PMv; peak value at time-zero lag. For each, left. Before injection of muscimol, center. One hour after the first injection of muscimol into the right M1, right. One hour after the second injection of muscimol into the left PMv. Fig.18 was illustrated in the same arrangement as Fig.9.

Fig.19 Schematic drawings of mirror movements suggested by the present results. A. Before blockade of M1 activity. B. After blockade of right M1. Thickness of the colored lines and arrows indicate the strength of activation.

Fig.1

A. Uncrossed corticospinal pathway

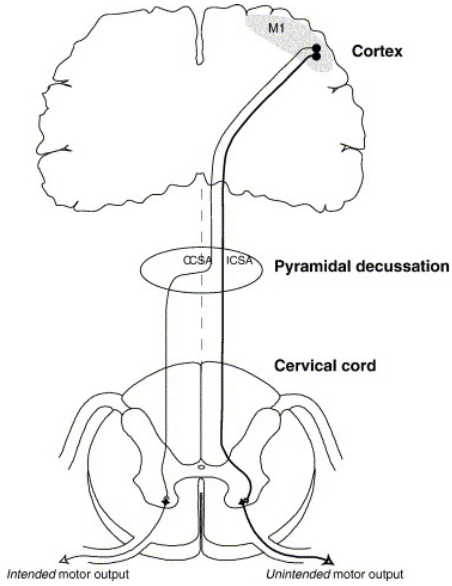

B. Branched bilateral corticomotoneuronal projections

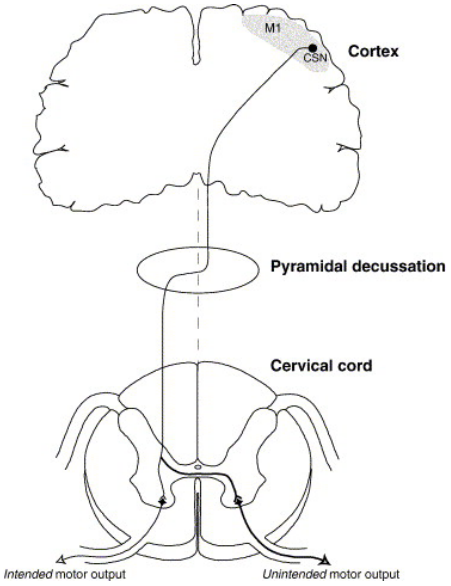

C. Collaterals of corticospinal neurons

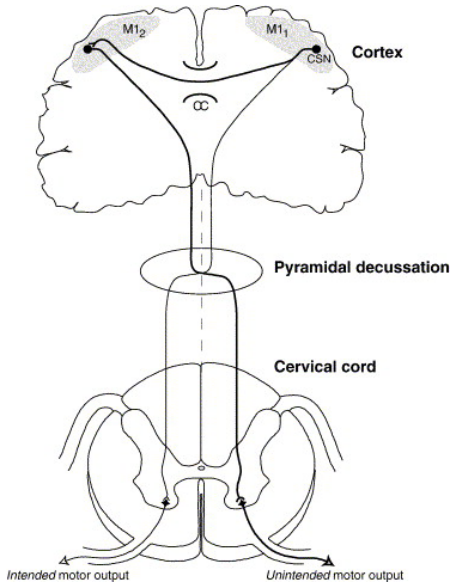

D. Common inputs to both motor cortex

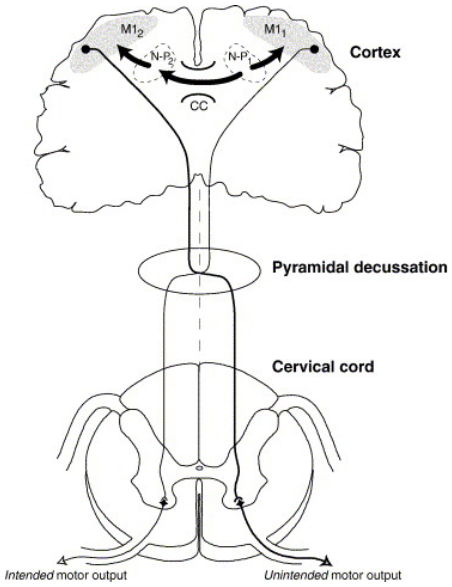

Fig.2

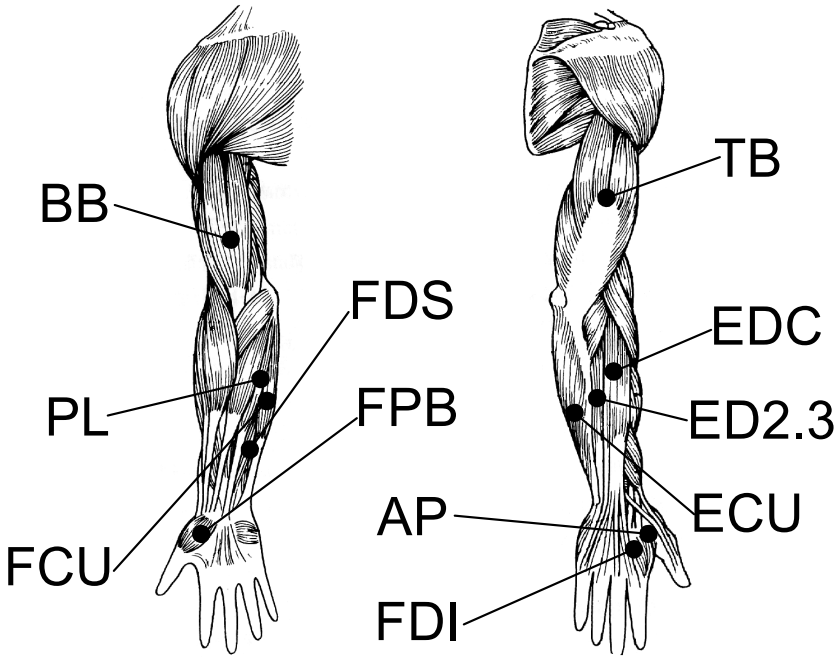

Fig.3

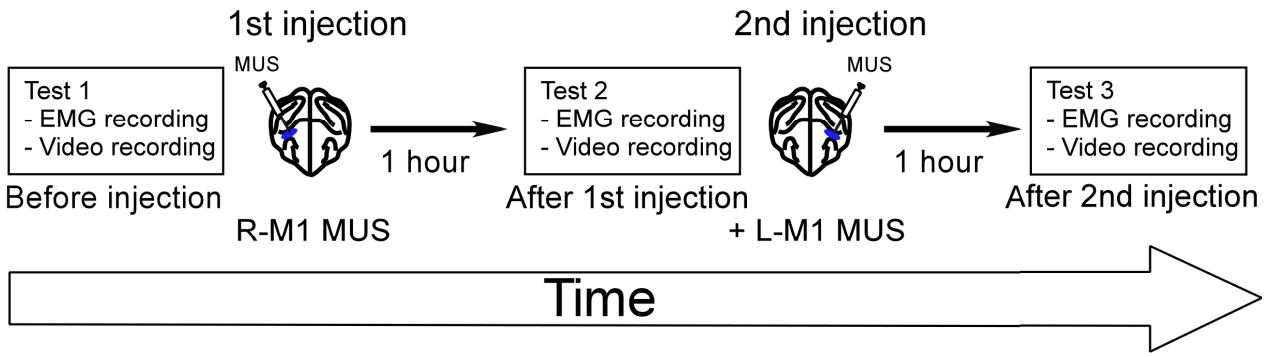
1st injection
2nd injection
MUS
MUS
Test 1
- EMG recording
- Video recording
1 hour
Test 2
- EMG recording
- Video recording
1 hour
Test 3
- EMG recording
- Video recording
Before injection
After 1st injection
After 2nd injection
R-M1 MUS
+ L-M1 MUS
Time

Fig.4

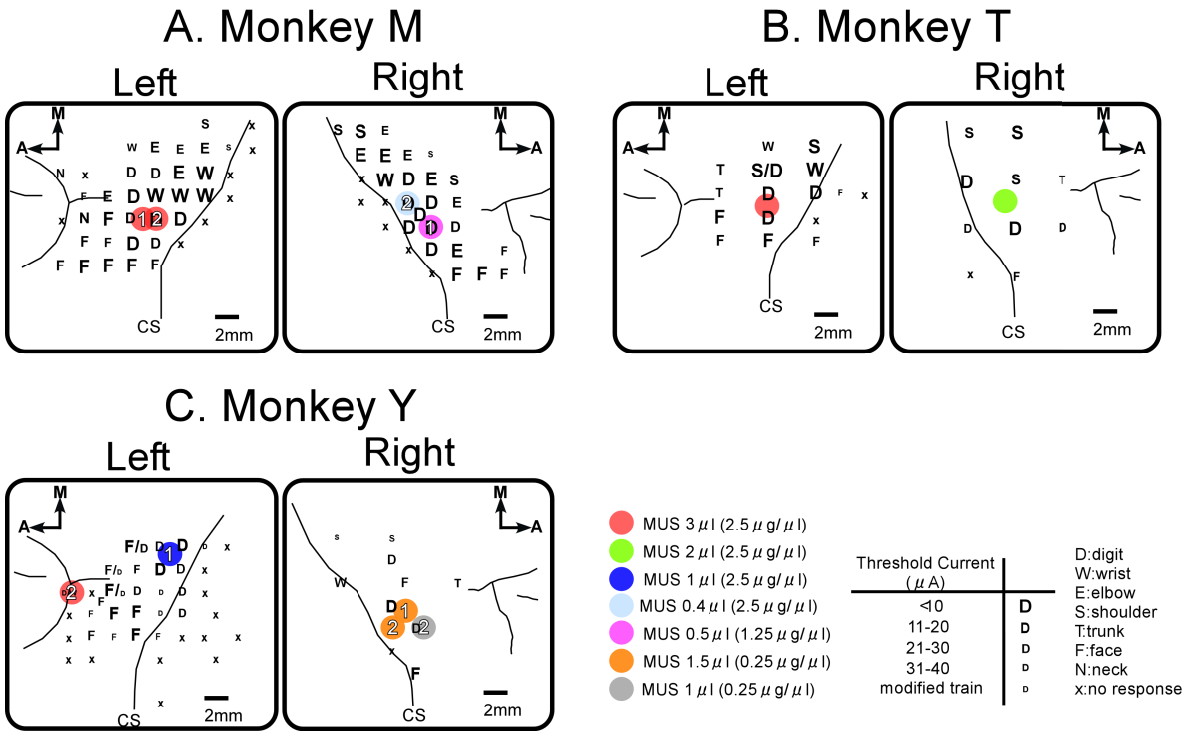
A. Monkey M
Left
Right
B. Monkey T
Left
Right
C. Monkey Y
Left
Right
M
A
CS
2mm
MUS 3 μl (2.5 μg/μl)
MUS 2 μl (2.5 μg/μl)
MUS 1 μl (2.5 μg/μl)
MUS 0.4 μl (2.5 μg/μl)
MUS 0.5 μl (1.25 μg/μl)
MUS 1.5 μl (0.25 μg/μl)
MUS 1 μl (0.25 μg/μl)
Threshold Current (μA)
<10
11-20
21-30
31-40
modified train
D:digit
W:wrist
E:elbow
S:shoulder
T:trunk
F:face
N:neck
x:no response

Fig.5

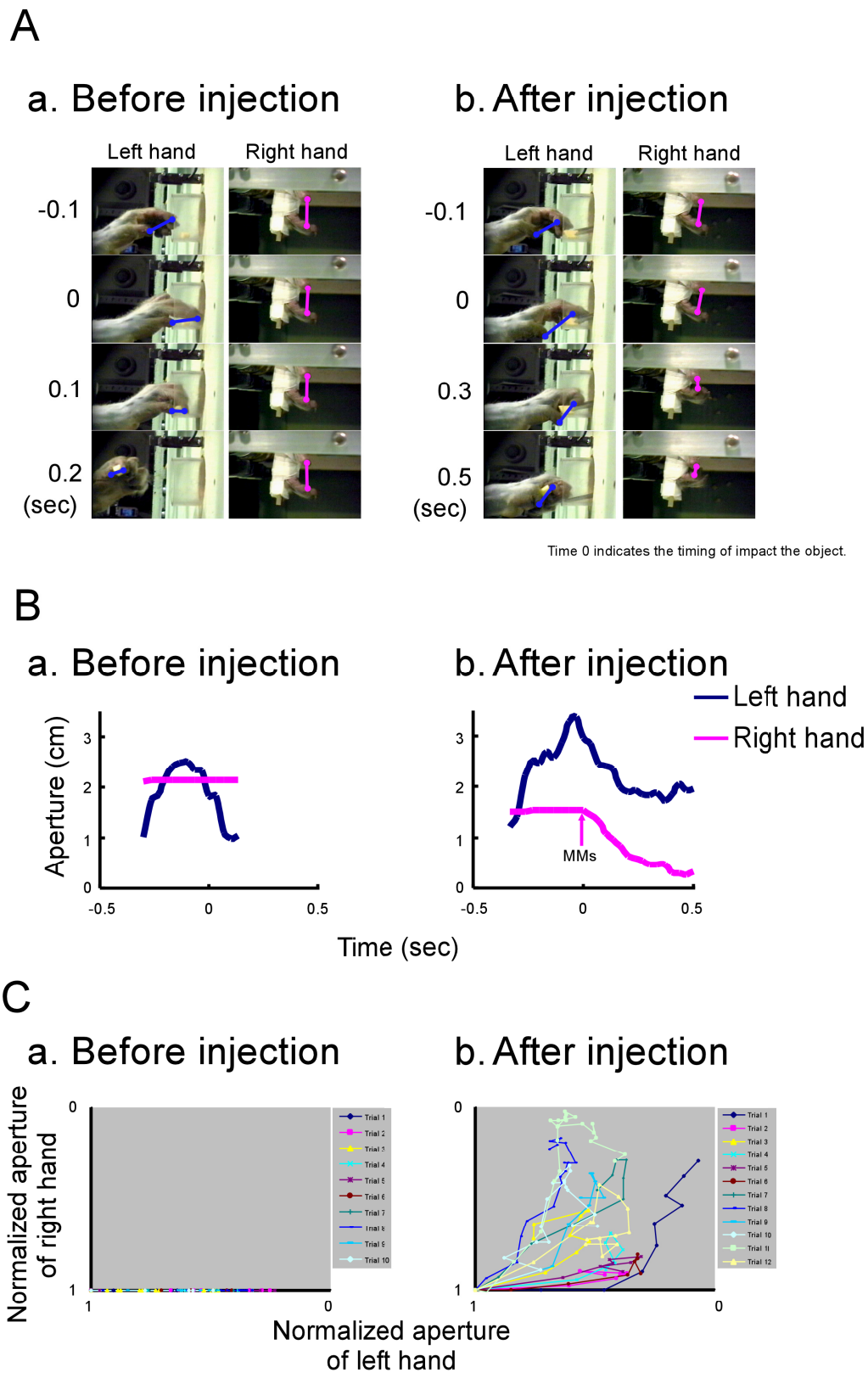
A
a. Before injection
b. After injection
Left hand
Right hand
-0.1
0
0.1
0.2
(sec)
0.3
0.5
Time 0 indicates the timing of impact the object.
B
Aperture (cm)
MMs
Left hand
Right hand
Time (sec)
C
Normalized aperture of right hand
Normalized aperture of left hand

Fig.6

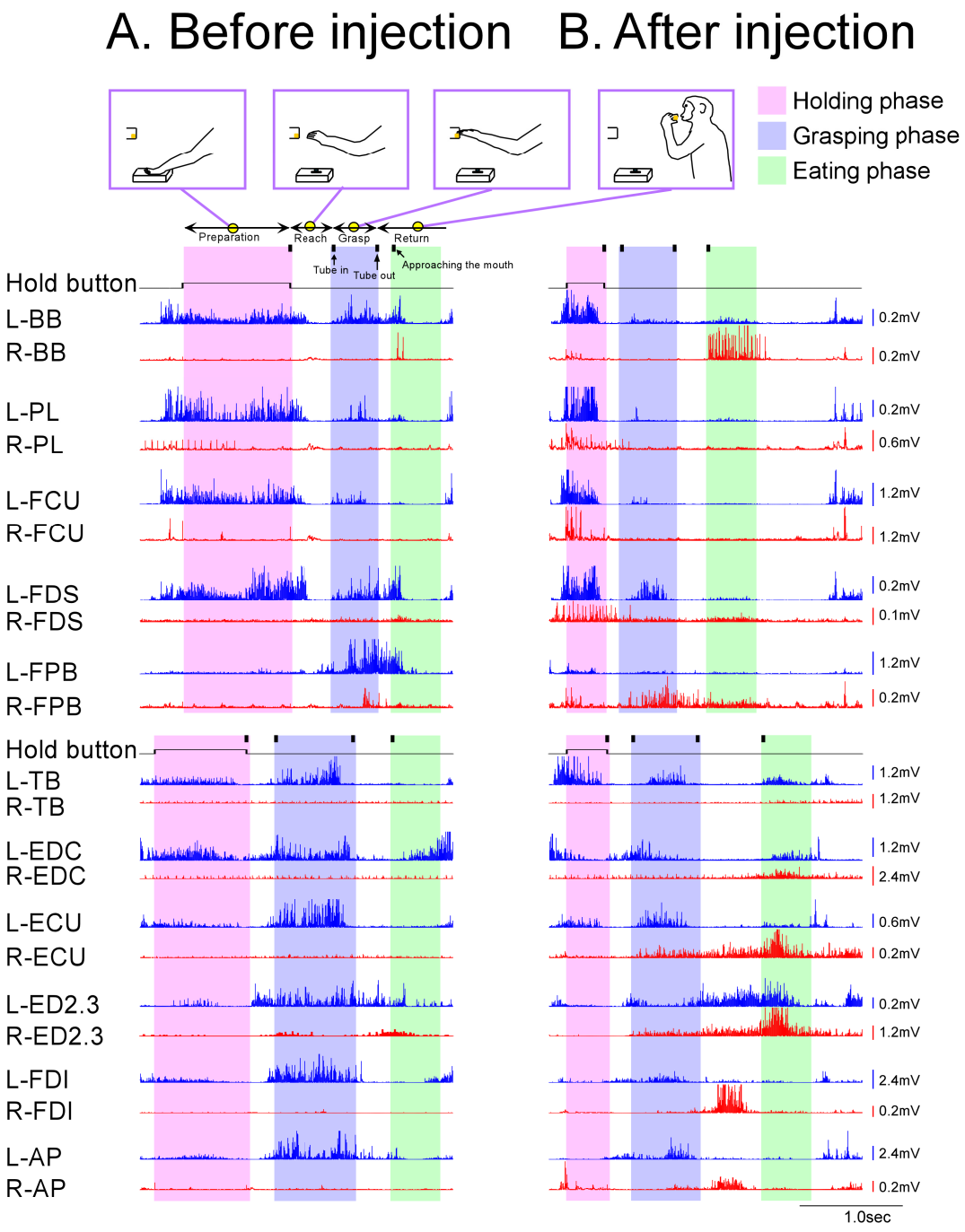
A. Before injection
B. After injection
Holding phase
Grasping phase
Eating phase
Preparation
Reach
Grasp
Return
Tube in
Tube out
Approaching the mouth
Hold button
L-BB
R-BB
L-PL
R-PL
L-FCU
R-FCU
L-FDS
R-FDS
L-FPB
R-FPB
Hold button
L-TB
R-TB
L-EDC
R-EDC
L-ECU
R-ECU
L-ED2.3
R-ED2.3
L-FDI
R-FDI
L-AP
R-AP
0.2mV
0.2mV
0.2mV
0.6mV
1.2mV
1.2mV
0.2mV
0.1mV
1.2mV
0.2mV
1.2mV
1.2mV
1.2mV
2.4mV
0.6mV
0.2mV
0.2mV
1.2mV
2.4mV
0.2mV
2.4mV
0.2mV
1.0sec

Fig.7

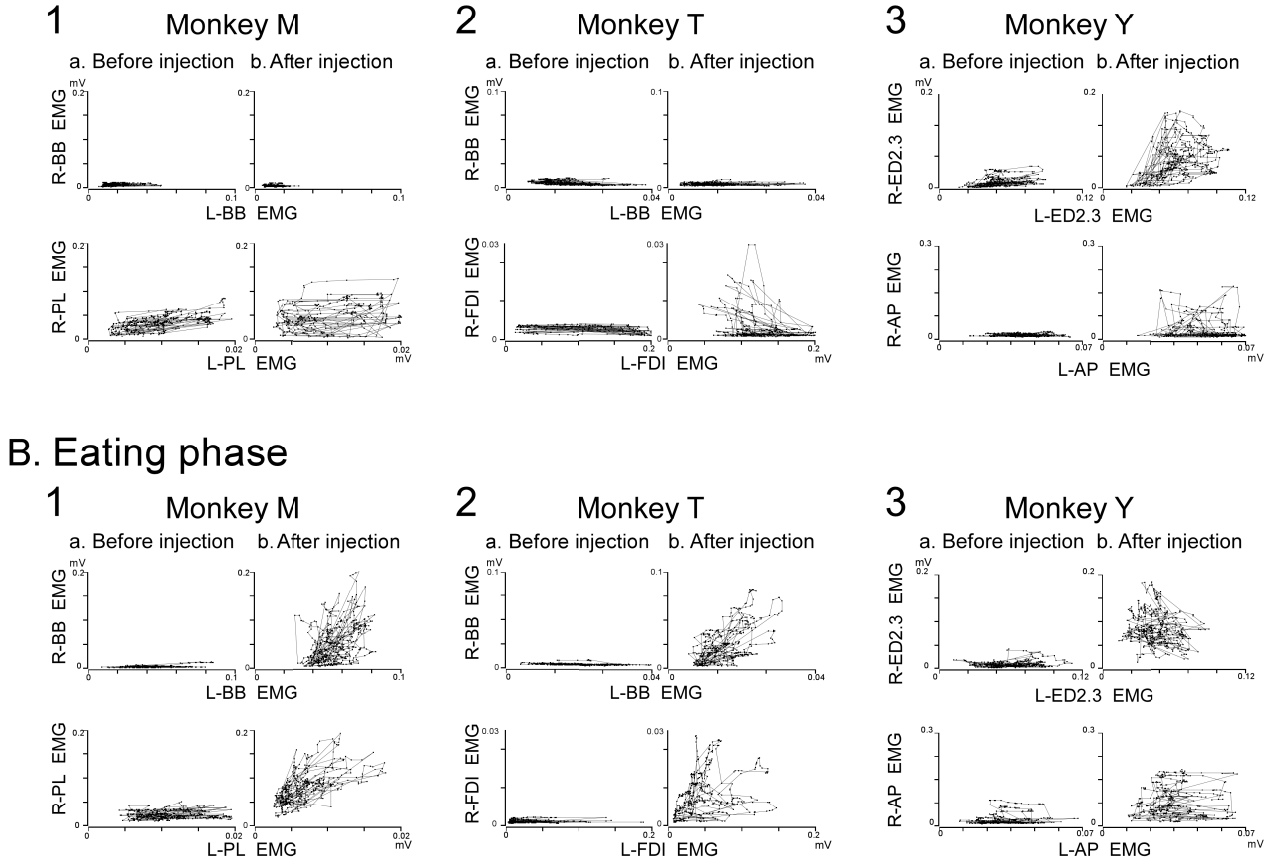
A. Grasping phase
1
Monkey M
a. Before injection
b. After injection
R-BB EMG
L-BB EMG
R-PL EMG
L-PL EMG
2
Monkey T
a. Before injection
b. After injection
R-BB EMG
L-BB EMG
R-FDI EMG
L-FDI EMG
3
Monkey Y
a. Before injection
b. After injection
R-ED2.3 EMG
L-ED2.3 EMG
R-AP EMG
L-AP EMG
B. Eating phase
1
Monkey M
a. Before injection
b. After injection
R-BB EMG
L-BB EMG
R-PL EMG
L-PL EMG
2
Monkey T
a. Before injection
b. After injection
R-BB EMG
L-BB EMG
R-FDI EMG
L-FDI EMG
3
Monkey Y
a. Before injection
b. After injection
R-ED2.3 EMG
L-ED2.3 EMG
R-AP EMG
L-AP EMG

Fig.8

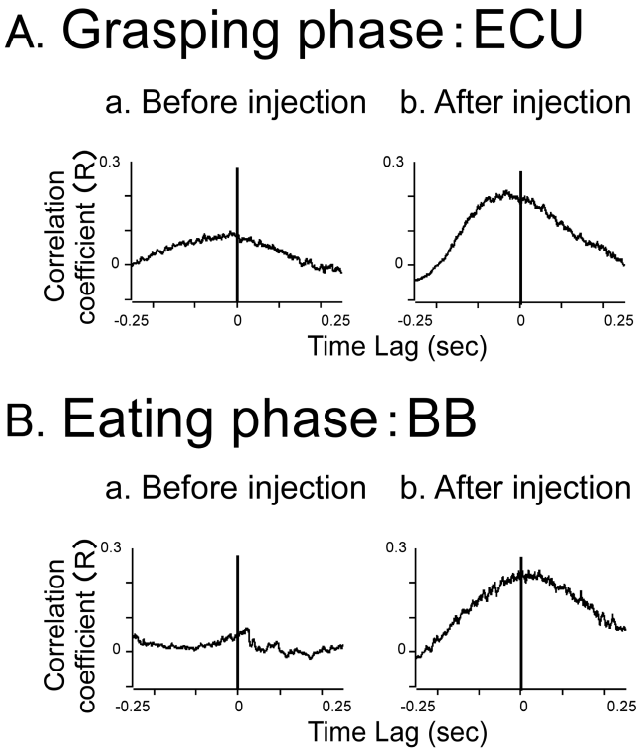
A. Grasping phase : ECU
a. Before injection
b. After injection
Correlation coefficient (R)
0.3
0
-0.25
0
0.25
Time Lag (sec)
B. Eating phase : BB
a. Before injection
b. After injection
Correlation coefficient (R)
0.3
0
-0.25
0
0.25
Time Lag (sec)

Fig.9

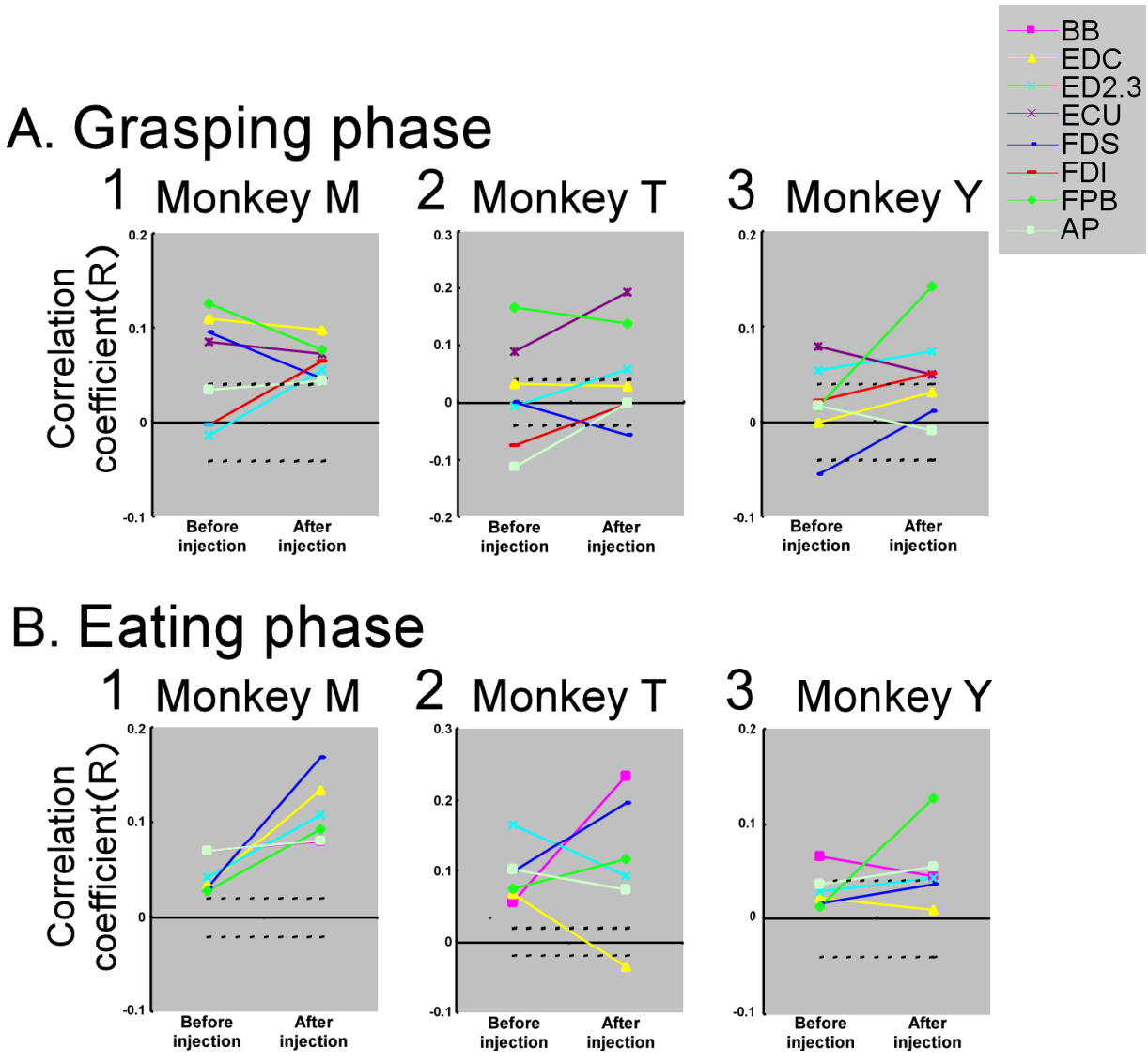
BB
EDC
ED2.3
ECU
FDS
FDI
FPB
AP
A. Grasping phase
1 Monkey M
2 Monkey T
3 Monkey Y
Correlation coefficient(R)
Before injection
After injection
B. Eating phase
1 Monkey M
2 Monkey T
3 Monkey Y
Correlation coefficient(R)
Before injection
After injection

Fig.10

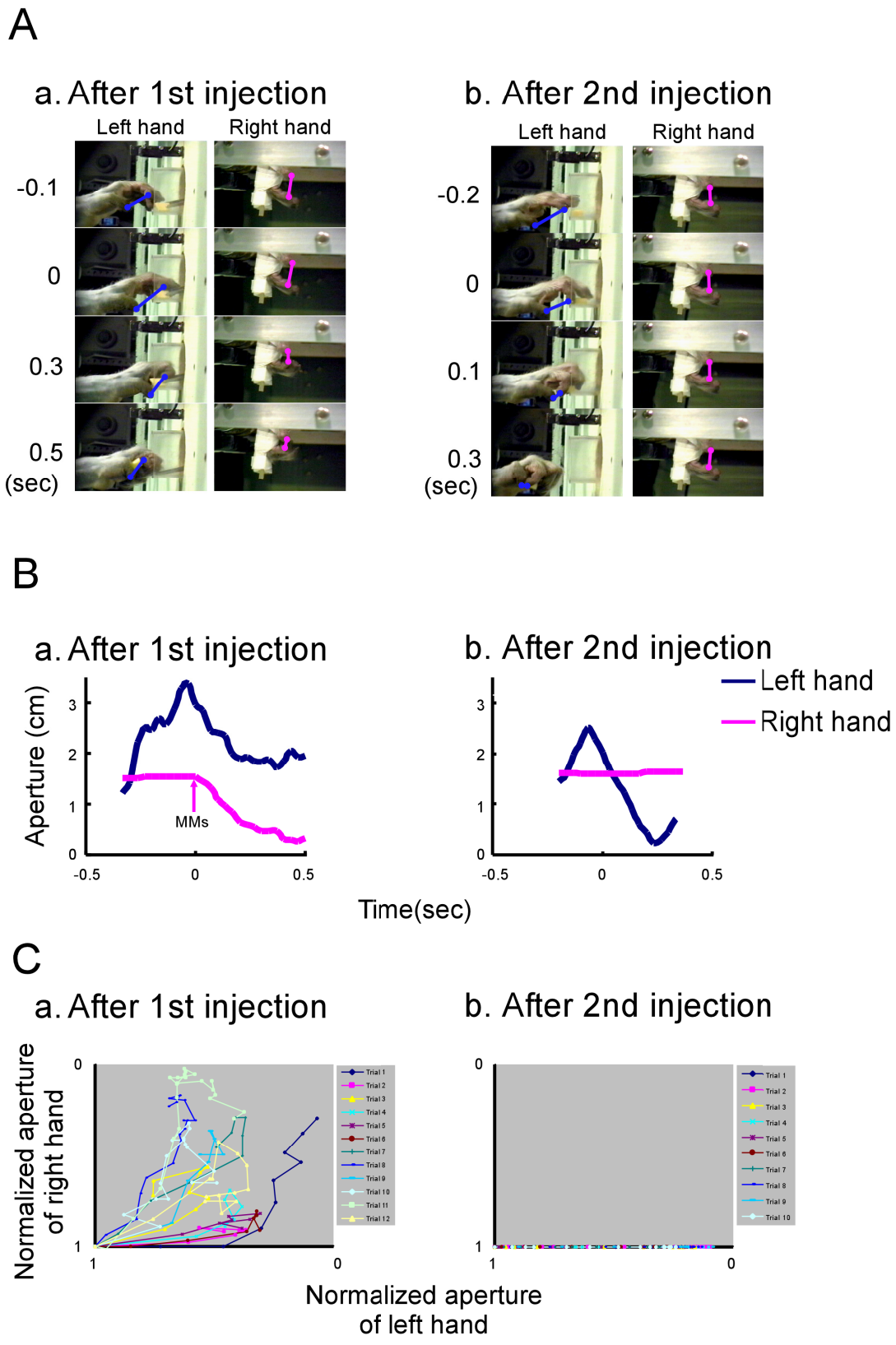
A
a. After 1st injection
Left hand
Right hand
-0.1
0
0.3
0.5
(sec)
b. After 2nd injection
Left hand
Right hand
-0.2
0
0.1
0.3
(sec)
B
a. After 1st injection
b. After 2nd injection
Left hand
Right hand
Aperture (cm)
MMs
Time(sec)
C
a. After 1st injection
b. After 2nd injection
Normalized aperture of right hand
Normalized aperture of left hand

Fig.11

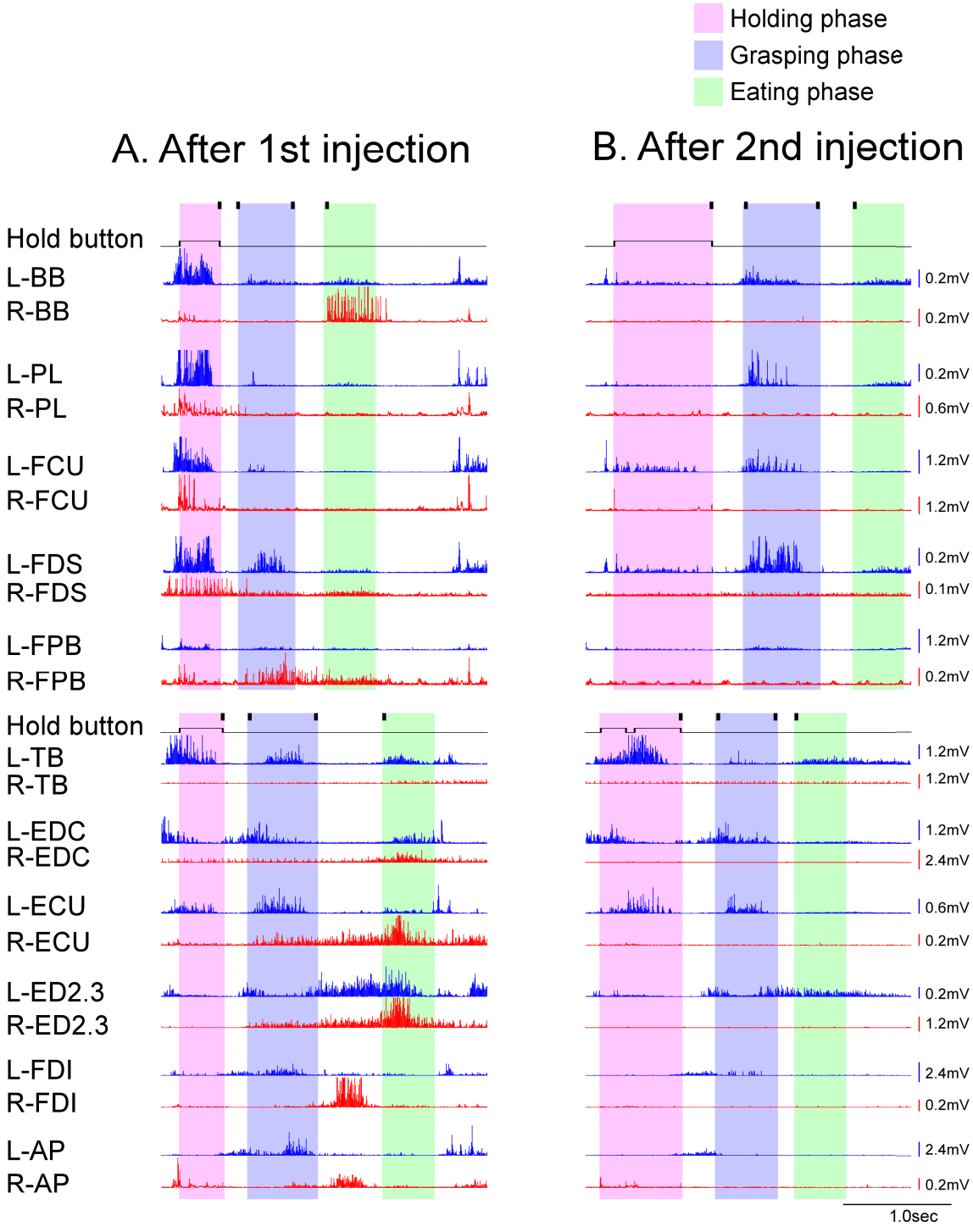
Holding phase
Grasping phase
Eating phase
A. After 1st injection
B. After 2nd injection
Hold button
L-BB
R-BB
L-PL
R-PL
L-FCU
R-FCU
L-FDS
R-FDS
L-FPB
R-FPB
Hold button
L-TB
R-TB
L-EDC
R-EDC
L-ECU
R-ECU
L-ED2.3
R-ED2.3
L-FDI
R-FDI
L-AP
R-AP
0.2mV
0.2mV
0.2mV
0.6mV
1.2mV
1.2mV
0.2mV
0.1mV
1.2mV
0.2mV
1.2mV
1.2mV
1.2mV
2.4mV
0.6mV
0.2mV
0.2mV
1.2mV
2.4mV
0.2mV
2.4mV
0.2mV
1.0sec

Fig.12

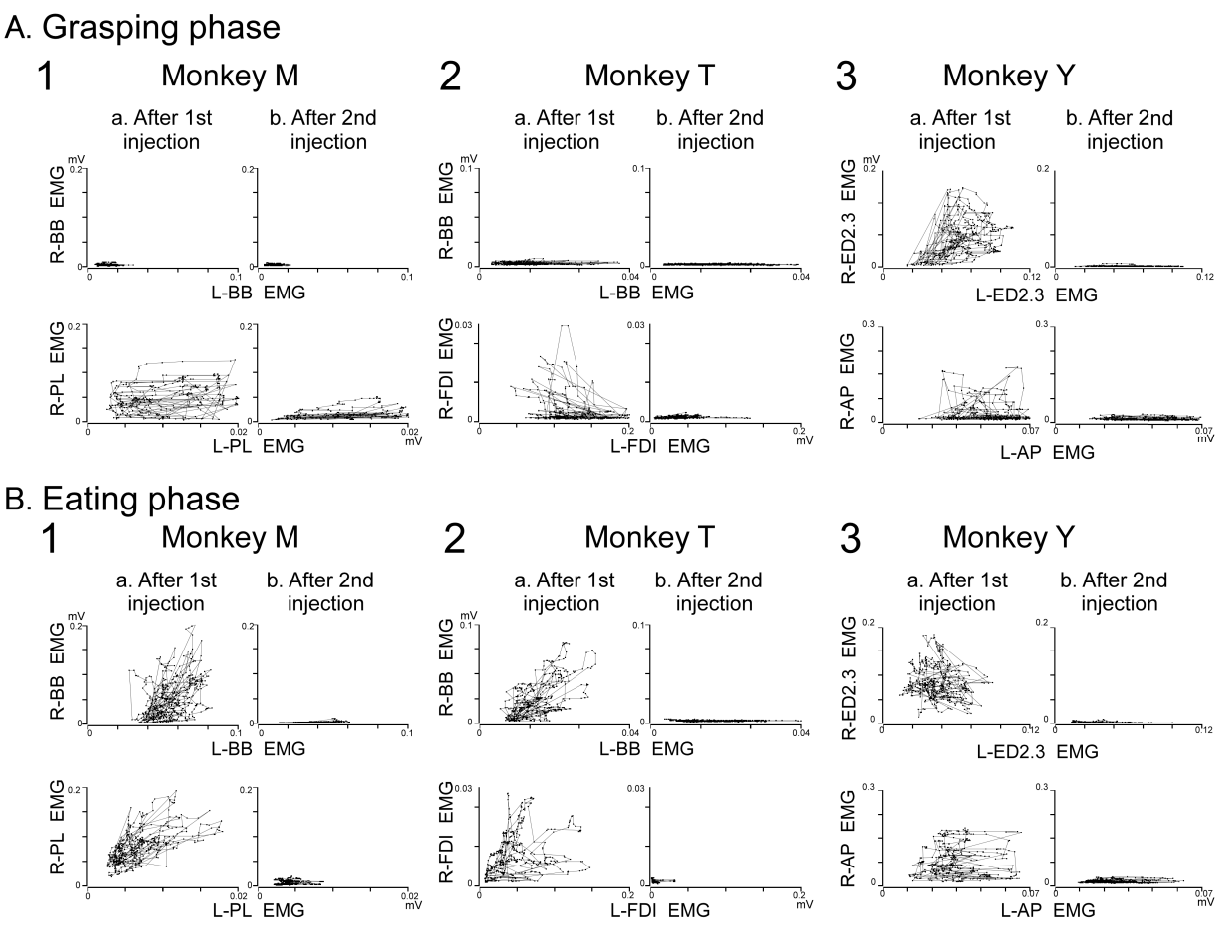
A. Grasping phase
1
Monkey M
2
Monkey T
3
Monkey Y
a. After 1st injection
b. After 2nd injection
R-BB EMG
L-BB EMG
R-PL EMG
L-PL EMG
R-FDI EMG
L-FDI EMG
R-ED2.3 EMG
L-ED2.3 EMG
R-AP EMG
L-AP EMG
mV
B. Eating phase
1
Monkey M
2
Monkey T
3
Monkey Y
a. After 1st injection
b. After 2nd injection
R-BB EMG
L-BB EMG
R-PL EMG
L-PL EMG
R-FDI EMG
L-FDI EMG
R-ED2.3 EMG
L-ED2.3 EMG
R-AP EMG
L-AP EMG
mV

Fig.13

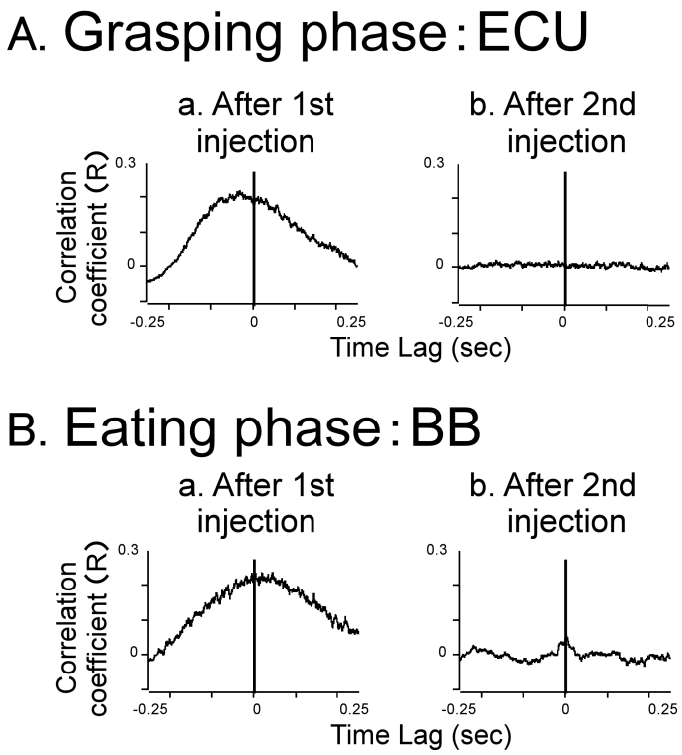
A. Grasping phase : ECU
a. After 1st injection
b. After 2nd injection
Correlation coefficient (R)
0.3
0
-0.25
0
0.25
Time Lag (sec)
B. Eating phase : BB
a. After 1st injection
b. After 2nd injection
Correlation coefficient (R)
0.3
0
-0.25
0
0.25
Time Lag (sec)

Fig.14

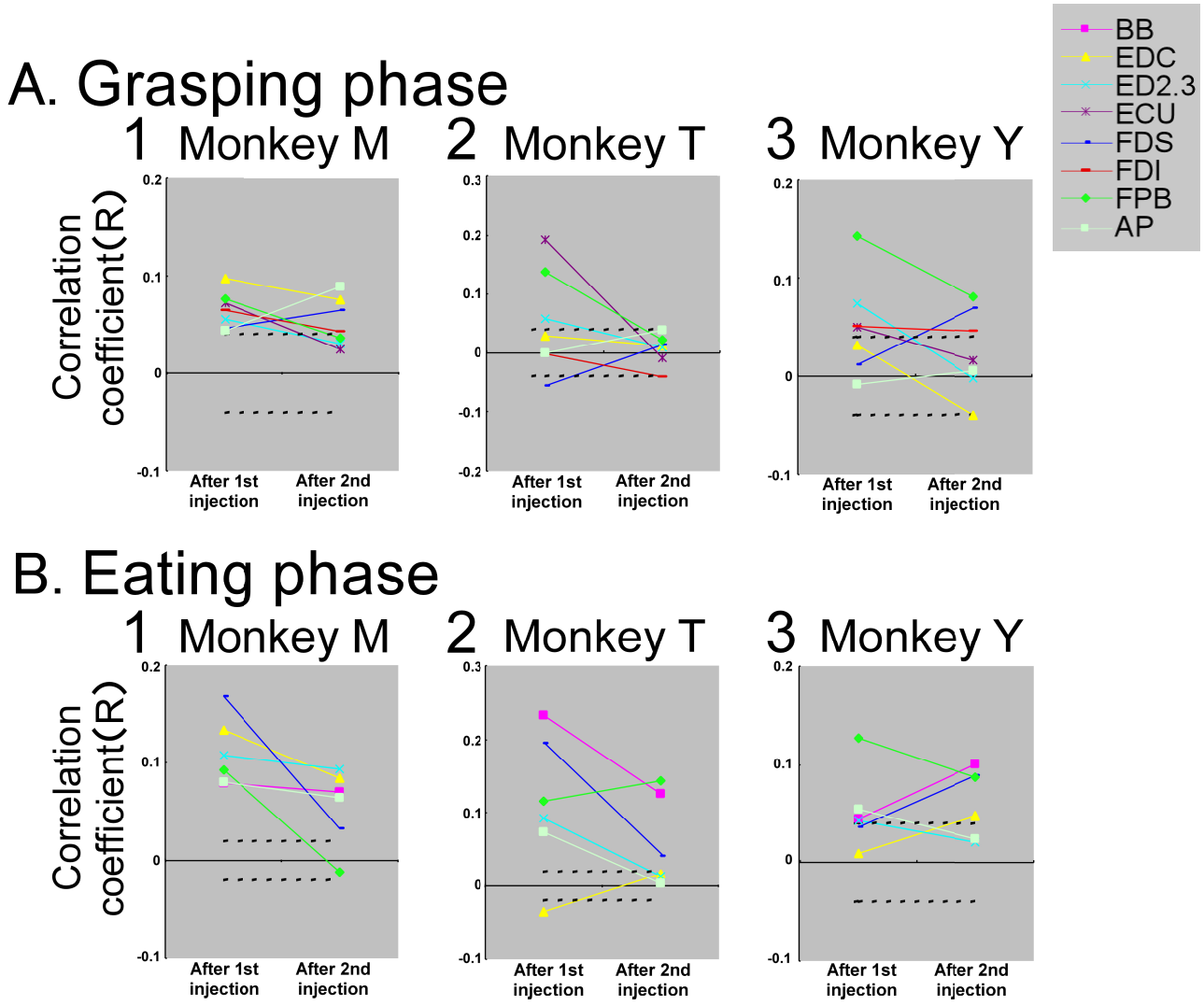
A. Grasping phase
1 Monkey M
2 Monkey T
3 Monkey Y
Correlation coefficient(R)
After 1st injection
After 2nd injection
B. Eating phase
1 Monkey M
2 Monkey T
3 Monkey Y
Correlation coefficient(R)
After 1st injection
After 2nd injection
BB
EDC
ED2.3
ECU
FDS
FDI
FPB
AP

Fig.15

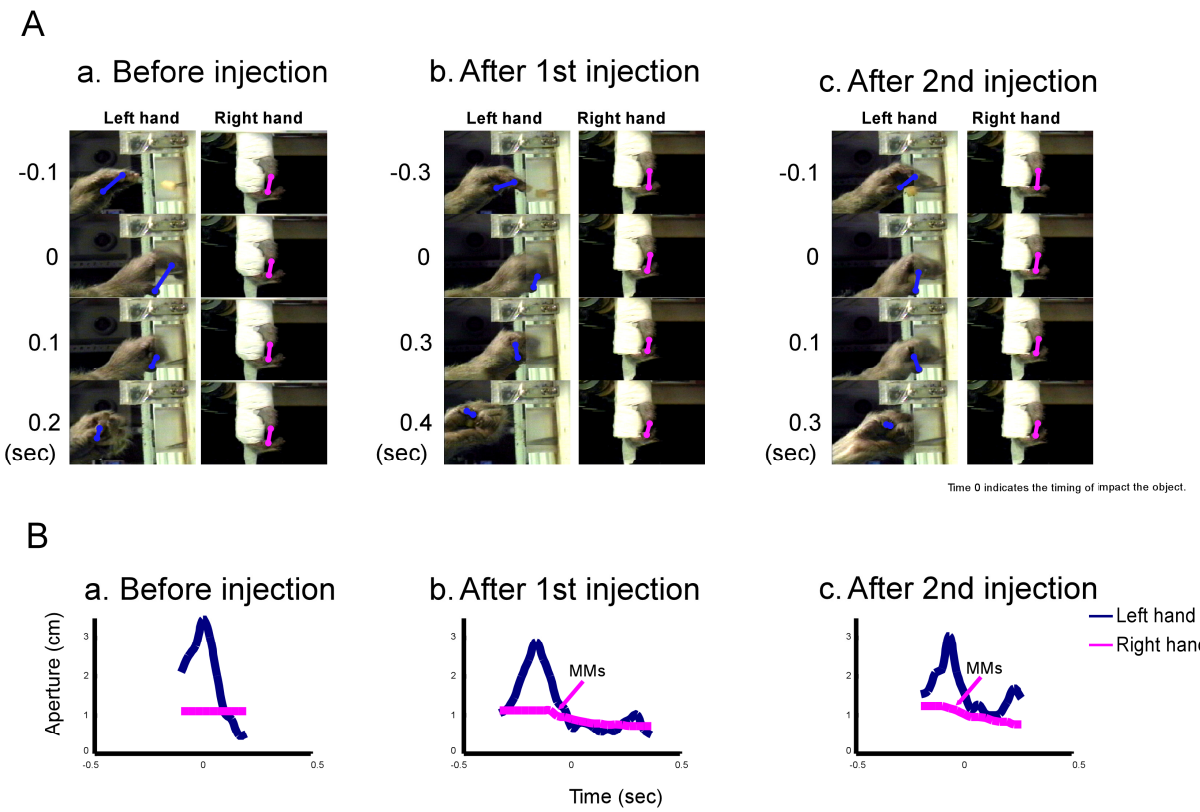
A
a. Before injection
b. After 1st injection
c. After 2nd injection
Left hand
Right hand
-0.1
0
0.1
0.2
(sec)
-0.3
0.3
0.4
0.3
Time 0 indicates the timing of impact the object.
B
Aperture (cm)
MMs
Time (sec)
Left hand
Right hand

Fig.16

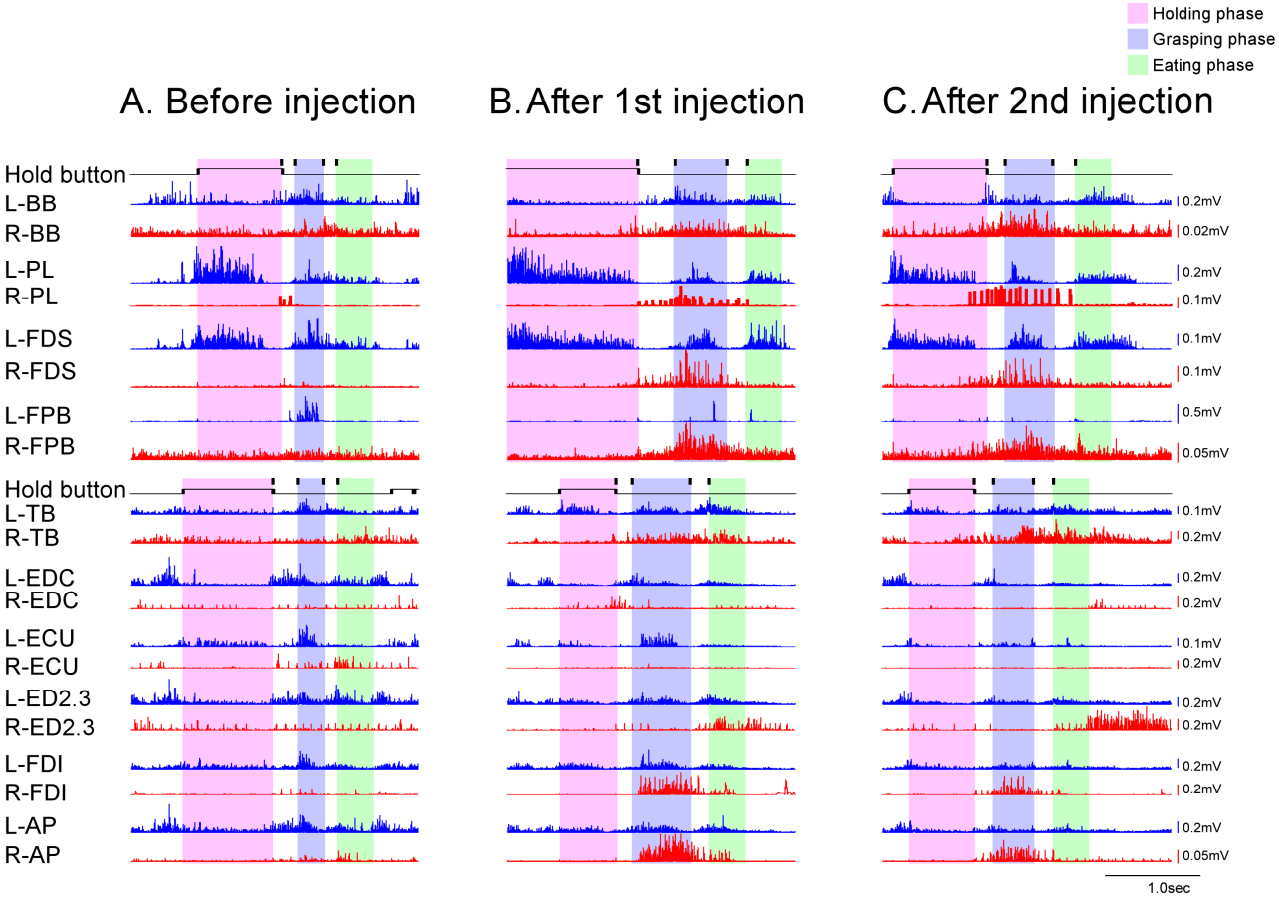
Holding phase
Grasping phase
Eating phase
A. Before injection
B. After 1st injection
C. After 2nd injection
Hold button
L-BB
R-BB
L-PL
R-PL
L-FDS
R-FDS
L-FPB
R-FPB
Hold button
L-TB
R-TB
L-EDC
R-EDC
L-ECU
R-ECU
L-ED2.3
R-ED2.3
L-FDI
R-FDI
L-AP
R-AP
0.2mV
0.02mV
0.2mV
0.1mV
0.1mV
0.1mV
0.5mV
0.05mV
0.1mV
0.2mV
0.2mV
0.2mV
0.1mV
0.2mV
0.2mV
0.2mV
0.2mV
0.2mV
0.2mV
0.05mV
1.0sec

Fig.17

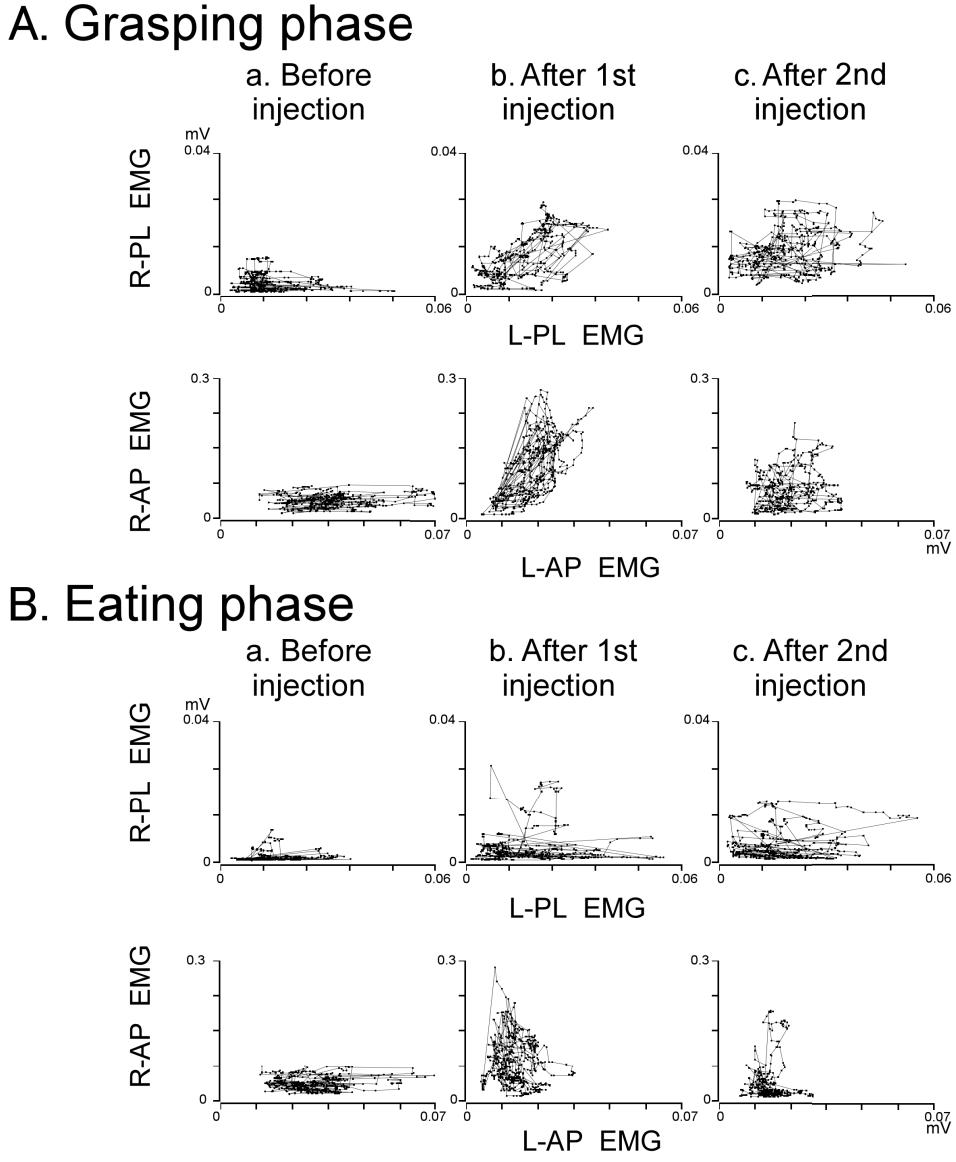
A. Grasping phase
a. Before injection
b. After 1st injection
c. After 2nd injection
mV
0.04
0
0.06
R-PL EMG
L-PL EMG
0.3
0.07
R-AP EMG
L-AP EMG
B. Eating phase

Fig.18

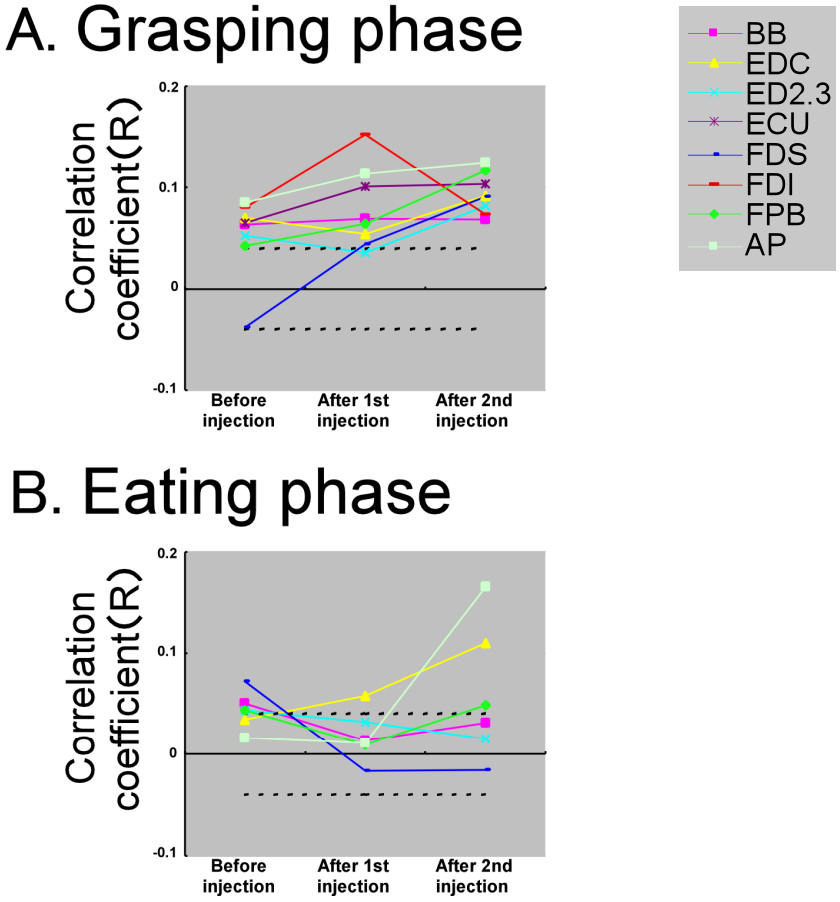
A. Grasping phase
Correlation coefficient(R)
0.2
0.1
0
-0.1
Before injection
After 1st injection
After 2nd injection
BB
EDC
ED2.3
ECU
FDS
FDI
FPB
AP
B. Eating phase
Correlation coefficient(R)
0.2
0.1
0
-0.1
Before injection
After 1st injection
After 2nd injection

Fig.19

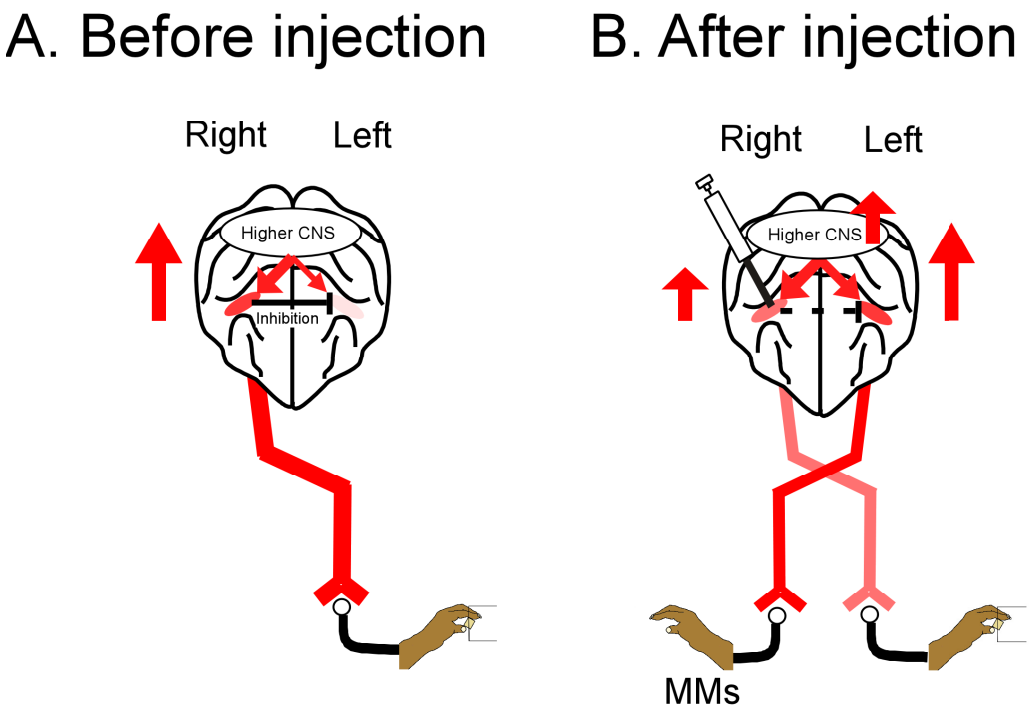
A. Before injection
B. After injection
Right
Left
Higher CNS
Inhibition
Right
Left
Higher CNS
MMs

References

Aranyi Z., Rosler K.M., (2002) Effort-induced mirror movements; A study of transcallosal inhibition in humans. Experimental Brain Research 145, 76-82

Brochier T., Boudreau M.J., Pare M., Smith A.M., (1999) The effects of muscimol inactivation of small regions of motor and somatosensory cortex on independent finger movements and force control in the precision grip. Experimental Brain Research 128, 31-40

Carson R.G. (2005) Neural pathways mediating bilateral interactions between the upper limbs. Brain Research Reviews 49, 641-662

Courtine G., Bunge M.B., Fawcett J.W., Grossman R.G., Kaas J.H., Lemon R., Maier I., Martin J., Nudo R.J., Ramon-Cueto A., Rouiller E.M., Schnell L., Wannier T., Schwab M.E., Edgerton V.R. (2007) Can experiments in nonhuman primates expedite the translation of treatments for spinal cord injury in humans? Nature Medicine 13 (5), 561-566

Darian-Smith C., Ciferri M.M. (2005) Loss and recovery of voluntary hand movements in the macaque following a cervical dorsal rhizotomy. Journal of Comparative Neurology 491(1), 27-45

Farmer S.F. (1990) Mirror movements studied in a patient with Klippel-Feil syndrome. Journal of Physiology 428, 467-484

Farmer S.F., Harrison L.M., Mayston M.J., Parekh A., James L.M., Stephens J.A. (2004) Abnormal cortex-muscle interactions in subjects with X-linked Kallmann's syndrome and mirror movements. Brain 127, 385-397

Isa T., Ohki Y., Alstermark B., Pettersson L.G., Sasaki S. (2007) Direct and indirect cortico-motoneuronal pathways and control of hand/arm movements. Physiology 22, 145-152

Kim Y.H., Jang S.H., Chang Y., Byun W.M., Son S., Ahn S.H. (2003) Bilateral primary sensori-motor cortex activation of post-stroke mirror movements: an fMRI study.

Neuroreport 14 (10), 1329-1332

Krams M., Quinton R., Mayston M.J., Harrison L.M., Dolan R.J., Bouloux P.M., Stephens J.A., Frackowiak R.S., Passingham R.E. (1997) Mirror movements in X-linked Kallmann's syndrome. II. A PET study. Brain 120 (7), 1217-1228

Lemon R.N., Griffiths J. (2005) Comparing the function of the corticospinal system in different species: organizational differences for motor specialization? Muscle & Nerve 32 (3), 261-279

Li J.Y., Espay A.J., Gunraj C.A., Pal P.P., Cunic D.C., Lang A.E., Chen R. (2007) Interhemispheric and ipsilateral connections in Parkinson's disease: relation to mirror movements. Movements Disorders 22 (6), 813-821

Mayston M.J., Harrison L.M., Stephens J.A. (1999) A nerurophysiological study of mirror movements in adults and children. Annals of Neurology 45 (5), 583-594

Mayston M.J., Harrison L.M., Quinton R., Stephens J.A., Krams M., Bouloux P.M. (1997) Mirror movements in X-linked Kallmann's syndrome. I. A neurophysiological study. Brain 120 (7), 1199-1216

Nass R. (1985) Mirror movement asymmetries in congenital hemiparesis: the inhibition hypothesis revisited. Neurology 35, 1059-1062

Nelles G., Cramer S.C., Schaechter J.D., Kaplan J.D., Finklestein S.P. (1998) Quantitative assessment of mirror movements after stroke. Stroke 29, 1182-1187

Nishimura Y., Morichika Y. and Isa T. (2009) A subcortical oscillatory network contributes to recovery of hand dexterity after spinal cord injury. Brain, in press

Ueki Y., Mima T., Oga T., Ikeda A., Hitomi T., Fukuyama H., Nagamine T. (2005) Dominance of ipsilateral corticospinal pathway in congenital mirror movements. Journal of Neurology, Neurosurgery & Psychiatry 76 (2), 276-279

Uttner I., Mai N., Esslinger O. and Danek A., (2005) Quantitative evaluation of mirror movements in adults with focal brain lesions. European Journal of Neurology 12,

964-975

Shibasaki H, Nagae K (1984) Mirror movement:application of movement-related cortical potentials. Annals of Neurology 15, 299-302

Verstynen T., Spencer R., Stinear C.M., Konkle T., Diedrichsen J., Byblow W.D., Ivry R.B. (2007) Ipsilateral corticospinal projections do not predict congenital mirror movements: A case report. Neuropsychologia 45 (4), 844-852

Acknowledgements

This study is supported by a lot of backups. I am deeply grateful to Professor Tadashi Isa at NIPS, for instructing and encouraging me throughout my graduate school years.

I also thank Dr. Yukio Nishimura at University of Washington, USA, who supported the experimental setup and electrophysiological technique.

I would like to thank Mr. Yosuke Morichika who taught me how to care the monkey.

I would like to thank all the member of Department of Developmental Physiology, NIPS, and the member of Isa's group supported by CREST of Japan Science and Technology Agency.

Finally, I would like to thank my parents for economical support my graduate school years.